Talanta 103 (2013) 86–94

Contents lists available at SciVerse ScienceDirect

Talanta

journal homepage: www.elsevier.com/locate/talanta

# Simultaneous determination of plant growth regulators in environmental samples using chemometrics-assisted excitation–emission matrix fluorescence: Experimental study on the prediction quality of second-order calibration method

Xiang-Dong Qing, Hai-Long Wu*, Chong-Chong Nie, Xiu-Fang Yan, Yuan-Na Li, Jian-Yao Wang, Ru-Qin Yu

*State Key Laboratory of Chemo/Biosensing and Chemometrics, College of Chemistry and Chemical Engineering, Hunan University, Changsha 410082, China*

ARTICLE INFO

*Article history:*
Received 17 June 2012
Received in revised form
26 September 2012
Accepted 5 October 2012
Available online 12 October 2012

*Keywords:*
Second-order calibration
SWATLD
Excitation–emission matrix fluorescence
2-naphthoxyacetic acid
1-naphthaleneacetic acid methyl ester
Environmental sample

ABSTRACT

In this work, with the purpose of developing an effective and inexpensive method, excitation–emission matrix fluorescence data and second-order calibration method based on the self-weighted alternating trilinear decomposition (SWATLD) algorithm were combined for simultaneous determination of 2-naphthoxyacetic acid (NOA) and 1-naphthaleneacetic acid methyl ester (NAAME) in environmental samples, *i.e.* soil and sewage samples. In order to investigate the prediction quality of the proposed method, different strategies, such as taking spectroscopic measurements in the presence of different matrix interferents and at different fluorescence spectrophotometers, were introduced to build calibration models and comparisons among them were done subsequently. The root-mean-square error of prediction and t-test were used to compare different SWATLD-based calibration models. The limits of detection obtained for NOA and NAAME were 0.36–0.95 ng $mL^{-1}$ and 1.32–2.69 ng $mL^{-1}$, respectively, for different models. Such a chemometrics-based protocol may possess great potential to be extended as a promising alternative for more practical applications in environment monitoring and for the design of small intelligent and field-portable analytical instruments that rely on statistical discrimination, not complete instrumental separation, of the target analytes even in the presence of unknown and uncalibrated interferences.



## 1. Introduction

The combination of hyphenated instruments and second-order calibration methods are gaining widespread acceptance by the analytical community. Second-order calibration methods allow concentrations and spectral information of the sample components to be extracted from complicated spectroscopic measurements even in the presence of unknown interferents. This property, named the "second-order advantage", is presently exploited in many scientific fields, such as chemistry, medicine, food, environmental and single-cell science, as can be seen from an explosion of relevant literatures [1–6]. In recent decades, a great variety of second-order calibration methods with the "second-order advantages" have been produced for a three-way data array. They can be classified into two types. One is based on computing the regression coefficients leading to prediction by combining data from calibration and test samples, with parallel factor analysis (PARAFAC) [7], generalized rank annihilation method (GRAM) [8], direct trilinear decomposition (DTLD) [9], alternating trilinear decomposition (ATLD) [10] and its variants (self-weighted alternating trilinear decomposition (SWATLD) [11] and alternating penalty trilinear decomposition (APTLD) [12]), and multivariate curve resolution-alternating least squares (MCR-ALS) [13] as the well-known examples. The other is built on estimating loadings from calibration data only and then calculating regression coefficients after the test sample enters the scene, including bilinear least squares (BLLS) [14], unfolded-partial least squares (U-PLS) [15], N-way partial least-squares (N-PLS) [16], unfolded-principal component analysis (U-PCA) [17] combined with residual bilinearization (RBL). Each type of second-order calibration methods has its own advantages for effectively processing three-way data in certain cases.

The prediction quality of these second-order calibration methods has been explored in some literature. In Ref. [18], nine daily models and three global models constructed with the PARAFAC algorithm to accurately predict samples measured on different

* Corresponding author. Tel./fax: +86 731 88821818.
*E-mail address:* hlwu@hnu.edu.cn (H.-L. Wu).

0039-9140/$ - see front matter © 2012 Elsevier B.V. All rights reserved.
http://dx.doi.org/10.1016/j.talanta.2012.10.012

days and by different analysts, have been compared by Giménez et al.; Rinnan et al. have investigated the prediction quality of second-order calibration as a function of the size of the calibration set, the number and degree of overlap of new interferents and the type and magnitude of noise [19]. The prediction quality for the single matrix model, the intra-day various matrices model and the global model have been investigated by the APTLD-based second-order calibration method by Li et al. [20]. However, there was no work reported in the literature on the comparison of the prediction quality of second-order calibration applying to analysis of three-way data obtained at different experimental conditions, such as taking spectroscopic measurements in the presence of different matrix interferents and at different fluorescence spectrophotometers.

Fluorescence spectroscopy is a technique widely applied in routine analysis in many scientific fields [21–23]. Owing to its high sensitivity, high signal-to-noise ratios, ease of use and simple equipment of instruments, fluorescence spectrophotometer presents a higher potential for its transformation in a portable instrument. However, because its spectroscopy covers a wide range of excitation and emission wavelengths, the signal of analytes of interest is inevitably overlapped with each other and with the matrix constitutes in complex mixtures. To extract useful chemical information from the fluorescence spectra, advanced mathematical treatment and analysis is required. Second-order calibration analysis of excitation–emission matrix fluorescence (EEMF) data is the key factor in developing robust analytical methods. Methods such as the SWATLD algorithm and the PARAFAC algorithm have been used for quantitative determination of various plant hormones in environmental samples [24,25].

2-Naphthoxyacetic acid (NOA, Fig. 1) and 1-naphthaleneacetic acid methyl ester (NAAME, Fig. 1) are important plant hormones by synthesis. Both are widely used to inhibit lateral bud growth and stimulate fruit growth from flowers and prevent flower dropping in agriculture [26]. The use of these plant hormones has led to their presence in fruits, soils and sewage waters. The potential toxicity of these compounds on humans or animals has raised the need for effective methods for their control. Casado-Terrones et al. have developed and compared a fluorescence and a phosphorescence optosensors for determining NOA in soil samples [27]; another analytical method, micelle-stabilised room temperature phosphorescence (MS-RTP), for simultaneous determination of 1-naphthylacetic acid and NOA in commercial technical formulations, fruit and vegetable samples has been proposed by Murillo Pulgarín et al. [26]; Ibrahim et al. have investigated NAAME as well as 65 different volatile metabolites of tomato fruits using gas chromatography/mass spectrometry (GC/MS) [28]. However, the method for simultaneous determination of NOA and NAAME in environmental samples, *i.e.* soil and sewage samples has not been reported in the literature so far.

In the present work, fluorescence spectrophotometer was fully utilized to obtain EEMF data of complex environmental samples. Subsequently, second-order calibration method based on the SWATLD algorithm was applied to extracted useful chemical information from the obtained data, with the purpose of developing an effective and inexpensive method for simultaneous determination of NOA and NAAME in soil and sewage samples. In order to investigate the prediction quality of the proposed method, different strategies, such as taking spectroscopic measurements in the presence of different matrix interferents and at different fluorescence spectrophotometers, were introduced to build calibration models and comparisons among them were done subsequently. The root-mean-square error of prediction and t-test were used to compare different SWATLD-based calibration models.

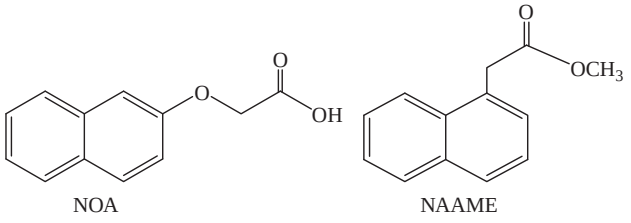


**Fig. 1.** Chemical structures of 2-naphthoxyacetic acid (NOA) and 1-naphthaleneacetic acid methyl ester (NAAME).

## 2. Theory

### 2.1. Trilinear component model for second-order calibration

Second-order data are usually generated from hyphenated instruments such as EEMF, liquid chromatography–mass spectrometry (LC–MS) and high performance liquid chromatography-diode array detection (HPLC-DAD). Suppose a given sample produces a data matrix of size $I \times J$, where $I$ and $J$ denote the number of data points in the first and second dimensions, respectively. Taking EEMF as an example, $I$ is the number of excitation wavelength data points and $J$ is the number of emission wavelength data points. If $K$ samples, consisting of calibration and prediction samples, are stacked, a three-way data array $\underline{\mathbf{X}}$ is obtained with dimensions $I \times J \times K$. A trilinear model for such a three-way array $\underline{\mathbf{X}}$ has the form:

$$x_{ijk} = \sum_{n=1}^{N} a_{in} b_{jn} c_{kn} + e_{ijk}, \quad i = 1,\ldots,I; \quad j = 1,\ldots,J; \quad k = 1,\cdots,K \tag{1}$$

Here $x_{ijk}$ is the element of $\underline{\mathbf{X}}$, $a_{in}$, $b_{jn}$ and $c_{kn}$ are the elements of the $I \times N$ matrix $\mathbf{A}$ corresponding to the emission spectral profiles, the $J \times N$ matrix $\mathbf{B}$ corresponding to excitation spectral profiles and the $K \times N$ matrix $\mathbf{C}$ corresponding to the relative concentrations, respectively. $e_{ijk}$ is the element of a three-way residual array $\underline{\mathbf{E}}$. $N$ denotes the number of factors, which is really the total number of detectable physically-meaningful components of interest as well as the interferents and the background.

### 2.2. SWATLD algorithm

The SWATLD algorithm was developed by our group as a derivative of the ATLD algorithm, which can yield better results in most cases. It is unique in that it alternately minimizes three different objective functions with intrinsic relationship and provides the features of fast convergence and being insensitivity to the excess factors used in calculation. Mathematical explanations of these valuable properties are presented by authors in original Ref. [11], so it is not described here.

## 3. Experimental

### 3.1. Reagents and chemicals

All of experiments were performed with analytical reagent grade chemicals, pure solvents and Milli-Q purified water. 2-Naphthoxyacetic acid (NOA, $\geq$98%) and 1-naphthaleneacetic acid methyl ester (NAAME, $\geq$98%) were obtained from Aladdin Chemistry Co., Ltd. (Shanghai, China). Sodium dodecyl sulphate (SDS) was purchased from Xilong Chemical Industry Incorporated Co., Ltd. (Shantou, China). The individual standard solutions of plant growth regulators were prepared by dissolving each compound in a small amount of methanol and then diluting in ultra pure water at appropriate concentrations and stored at 4 °C,

respectively. These stock solutions were stable for at least three days at room temperature. All the working aqueous solutions were prepared immediately before their use by taking appropriate aliquots of stock solutions and diluting with ultra pure water to the desired concentrations. The working solutions were stable for at least 3 days at room temperature. A stock solution of SDS containing 0.5 mol $L^{-1}$ was prepared by dissolving the compound in ultrapure water. Methanol was obtained from Tedia Company Incorporation (Fairfield, USA). Ultra pure deionized water with 18.20 MΩ $cm^{-1}$ was prepared using a Milli-Q water purification system (Millipore, USA).

### 3.2. Instrumentation and software

All of fluorescence measurements were carried out on three different F-4500 fluorescence spectrophotometers (Hitachi, Japan) according to the experimental requirements, each equipped with a continuous 150-W Xenon arc lamp and connected to a PC Celeron (R) microcomputer running under Windows XP (through a GPIB NI-488 interface). Data acquisition and analysis were performed by the use of software FL solution 2.0. In all cases, 1.0 cm quartz cells were used at room temperature. In the MATLAB environment all home-made programs were written and further used for data analysis. All of calculations were carried out on a microcomputer under the Microsoft Windows 7 operating system.

Instrumental parameter settings for three fluorescence spectrophotometers were monochromator slit widths, 5/5 nm; excitation wavelength, 200–308 nm (every 3 nm); emission wavelength, 308–392 nm (every 2 nm); scanning speed, 2400 nm $min^{-1}$; voltage, 700 V.

For a single sample, a matrix of size of $43 \times 37$ was obtained. The used spectral ranges were selected after a suitable consideration of the spectral regions corresponding to maximum signals for the analyte and avoiding useless background signals, such as Rayleigh and Raman scattering.

### 3.3. Sample collection and preparation

The soil samples were scooped out from the bank of the Xiangjiang River in Hunan Province of China and brought to the laboratory in plastic bags without any pretreatment. The sewage samples were collected from a sewer in residential area in Changsha, China. The soil samples were dried at room temperature, and ground with a mortar. Then, 100 g soil samples were obtained and 100 mL of methanol were added, then, the mixture was vortexed for 30 min and left for a whole day in order to extract adequately. The mixture was filtered and the solvent was evaporated to dryness. The residue was reconstituted with 100 mL ultrapure water. The 100 mL sewage was filtered through filter paper to remove suspended sediments and solid materials. Then the soil extract and sewage filtrate were sterilized in autoclave.

### 3.4. Prediction models

Six initial different models for performing second-order prediction using the SWATLD algorithm were built successively. These were reduced to three different types of sample sets for reasons explained below.

#### 3.4.1. Validation sample set

A 18-samples set, containing 8 calibration samples and 10 test samples, was constructed as validation set to validate the performance of second-order calibration based on the SWATLD algorithm. These samples only contained two analytes without interferents.

**Table 1**
Added volumes of NOA and NAAME in validation, soil and sewage samples.

| Sample no. | Added volume (mL) | |
|---|---|---|
| | NOA | NAAME |
| Calibration | | |
| C1 | 2.00 | 0 |
| C2 | 0 | 2.00 |
| C3 | 1.90 | 0.10 |
| C4 | 0.10 | 1.80 |
| C5 | 1.50 | 0.50 |
| C6 | 0.50 | 1.30 |
| C7 | 1.00 | 0.90 |
| C8 | 0.80 | 1.10 |
| Test | | |
| T1 | 1.75 | 0.15 |
| T2 | 0.35 | 1.95 |
| T3 | 1.35 | 0.35 |
| T4 | 1.95 | 1.85 |
| T5 | 1.55 | 0.55 |
| T6 | 0.55 | 1.35 |
| T7 | 1.15 | 0.95 |
| T8 | 0.85 | 1.15 |
| T9 | 1.85 | 0.75 |
| T10 | 0.15 | 1.55 |

Added volumes of NOA and NAAME in validation samples were shown in Table 1, where the concentration of stock standard solutions of NOA and NAAME were 272.0 ng $mL^{-1}$ and 686.0 ng $mL^{-1}$, respectively. The concentration levels corresponded to values in the range 0–54.4 ng $mL^{-1}$ for NOA and 0–137.6 ng $mL^{-1}$ for NAAME. 0.3 mL SDS, which was used as micellar agent to enhance the intensity of fluorescence of the analytes, was added to each solution. This validation model was coded as model 1.

#### 3.4.2. Soil sample sets

The fluorescent spectra of two soil sample sets were recorded at three different F4500 fluorescence spectrophotometers (F4500-1, F4500-2, F4500-3), respectively, according to the experimental requirements. The first soil samples were measured at F4500-1 and F4500-3, respectively and two data sets were obtained (models 2 and 6). Then, other two data sets were obtained by measured the second soil samples at F4500-1 and F4500-2 (models 4 and 5), respectively. Each soil sample set contained 21 samples, and the first eight samples (C1–C8) were constructed as a calibration set by adding appropriate stock solutions of the two analytes and 0.3 mL SDS into 10 mL volumetric flask and diluting to the mark with ultra pure water, respectively. Then, the next 10 samples (T1–T10) were prepared as a prediction set by spiking them with both analytes and 0.3 mL SDS, the concentrations of both analytes were selected at random from the corresponding calibration ranges. Added volumes of NOA and NAAME in soil samples were the same as validation samples (see Table 1), where the concentration of stock standard solutions of NOA and NAAME were 235.0 ng $mL^{-1}$ and 652.0 ng $mL^{-1}$, respectively. The concentration levels corresponded to values in the range 0–47.0 ng $mL^{-1}$ for NOA and 0–130.4 ng $mL^{-1}$ for NAAME. In addition, three different analytes-free soil blank samples were prepared for estimating the limits of detection.

#### 3.4.3. Sewage sample set

The building of sewage samples was done following a similar procedure to that described for the building of soil samples, a 21-samples data set was obtained by measured 8 calibration samples, 10 sewage samples and 3 analytes-free sewage blank samples at F4500-1 (model 3). The concentration of stock standard

**Table 2**
Results in prediction for six initial models by applying SWATLD before removing outlier samples.

| Initial model | Matrix interferent | Instrument | NOA | | | NAAME | | | Samples outlier/total |
|---|---|---|---|---|---|---|---|---|---|
| | | | AR[a] | t-Test[b] | RMSEP[c] | AR[a] | t-Test[b] | RMSEP[c] | |
| 1 | Without | F4500-1 | $99.0 \pm 4.9$ | 0.38 | 2.31 | $102.2 \pm 4.9$ | 1.04 | 4.64 | 1/10 |
| 2 | Soil extract | F4500-1 | $98.1 \pm 12.0$ | 0.26 | 7.97 | $106.5 \pm 10.7$ | 1.14 | 4.66 | 3/10 |
| 3 | Sewage filtrate | F4500-1 | $83.2 \pm 6.9$ | 4.44 | 5.22 | $99.8 \pm 4.1$ | 0.13 | 4.69 | 3/10 |
| 4 | Soil extract | F4500-1 | $95.1 \pm 5.4$ | 1.59 | 3.39 | $102.4 \pm 9.3$ | 0.58 | 6.89 | 2/10 |
| 5 | Soil extract | F4500-2 | $112.1 \pm 15.0$ | 1.40 | 2.16 | $108.5 \pm 9.5$ | 1.55 | 3.48 | 2/10 |
| 6 | Soil extract | F4500-3 | $76.2 \pm 9.0$ | 5.05 | 10.46 | $75.9 \pm 7.0$ | 6.01 | 16.55 | 10/10 |

[a] Average recovery, %.
[b] $t^9_{0.025} = 2.26$.
[c] RMSEP, the root-mean-square error of prediction can be calculated in terms of the formula as $\mathrm{RMSEP}=[1/(I-1)\sum(c_{act}-c_{pred})^2]^{1/2}$, where $I$ is the number of prediction samples, $c_{act}$ and $c_{pred}$ are the actual and predicted concentrations of the analytes, respectively, ng $mL^{-1}$.

solutions of NOA and NAAME were 298.0 ng $mL^{-1}$ and 722.0 ng $mL^{-1}$, respectively. The concentration levels corresponded to values in the range 0–59.6 ng $mL^{-1}$ for NOA and 0–144.4 ng $mL^{-1}$ for NAAME.

A summary was given in Table 2.

## 4. Results and discussion

Prior to the measurement, soil samples were converted into liquid form and sewage samples were used directly except for filtering the suspended solid materials and sediments. Such simple pretreatment is usually not selective enough, and often partial interfering matrices from environmental samples were co-extracted with the analytes of interest.

Fig. 2 showed three-dimensional plots of the EEMF spectra for pure analytes and environmental samples. As can be appreciated, heavy fluorescence overlapping between the analytes and the environmental background of the samples occurred in the chosen region, especially for soil matrix. It implied the difficulty in directly determining NOA and NAAME in actual complex mixtures with ordinary method. Alternatively, one can resort to the application of the second-order calibration method, which might light to a new avenue to replace the "physical or chemical separation" with "mathematical separation" strategy through separating the signals of target analyte(s) away from those of uncalibrated background or interferences. In the paper, the SWATLD algorithm was recommended to simultaneously assay the concentrations of NOA and NAAME in soil and sewage samples. Additionally, in order to investigate the prediction quality of SWATLD-based second-order calibration method, the effect of different matrix interferent and concentration-response difference among different fluorescence spectrophotometers had been investigated. The results would be discussed in detail in the following sections.

### 4.1. Validation model

Whether the adopted method can be applied to analysis of two plant growth regulators in environmental samples or not, method validation is possibly the most important step in the model building sequence, it is also one of the most overlooked. So model 1 was established to validate the performance of the method. The third line of Table 2 showed the results in prediction for model 1 by applying the SWATLD algorithm before removing outlier samples. Good recoveries were obtained in validation samples, and the RMSEPs were 2.31 ng $mL^{-1}$ for NOA and 4.64 ng $mL^{-1}$ for NAAME. A t-test was performed to compare the recoveries of two analytes with the ideal value of 100%, *i.e.* $T = (\overline{X}-\mu_0)/(S/\sqrt{n})$ , $\overline{X}$ is the average recovery, $\mu_0$ is 100%, $n$ is degree of freedom (where $n+1$ is the number of evaluated levels), confidence level is 95%. The null hypothesis is: "the average recovery is equal to 100%". Here $T \le t^9_{0.025} = 2.26$, that suggested that the results for NOA and NAAME were accurate and reliable.

The third line of Table 3 showed the results after removing outlier samples. It was clear that the results after removing outlier samples were better than the ones before treatment. So, it was necessary to remove outlier samples in each of previously processed datasets. Outlier samples detection is based on the following criterion: $||(c_{pred}-c_{act})/c_{act}|| \times 100\% > 15\%$, where $c_{pred}$ and $c_{act}$ are the predicted and actual concentrations of the analytes, respectively.

The results highlighted the fact that the method was reliable for the simultaneous determination of NOA and NAAME in validation samples.

### 4.2. Models based on different matrices

Once the validation model has been accepted, the proposed method could be used to investigate more complex problems of the potential presence of interfering components in nature matrix samples. Therefore, two experimental sets, one containing heavy fluorescence interfering components in the soil samples, the other existing matrix effects such as fluorescence quenching in the sewage samples, were firstly selected to investigate the prediction quality of the proposed method.

#### 4.2.1. Model for quantification of NOA and NAAME in soil samples

In the experiment, there were heavy fluorescence interfering components which produced serious spectral overlapping with the analytes (Fig. 2(c)), it was very suitably used to investigate the second-order advantage and prediction quality of the proposed method. So, model 2 was built for the purpose.

The core consistency diagnostic (CORCONDIA), which was proposed by Bro et al. [29], was employed to choose the optimum number of factors. In model-building, a four-component model was constructed according to the results from CORCONDIA. Then, the tensor obtained was decomposed by the SWATLD algorithm.

Fig. 3 showed the actual and resolved normalized excitation spectra, normalized emission spectra and relative concentration profiles of NOA and NAAME in soil samples. From the figure can be seen, a very high overlapping can be observed between the spectral profiles of NOA, NAAME and soil matrix. However, it was found that the spectral and concentration information of both analytes were simultaneously extracted from spectroscopic measurement of complex soil matrix.

The predicted concentrations as a function of the nominal values by applying the SWATLD algorithm to analysis of initial model 2 (green triangle up) were drawn in Fig. 4(a) and (c).

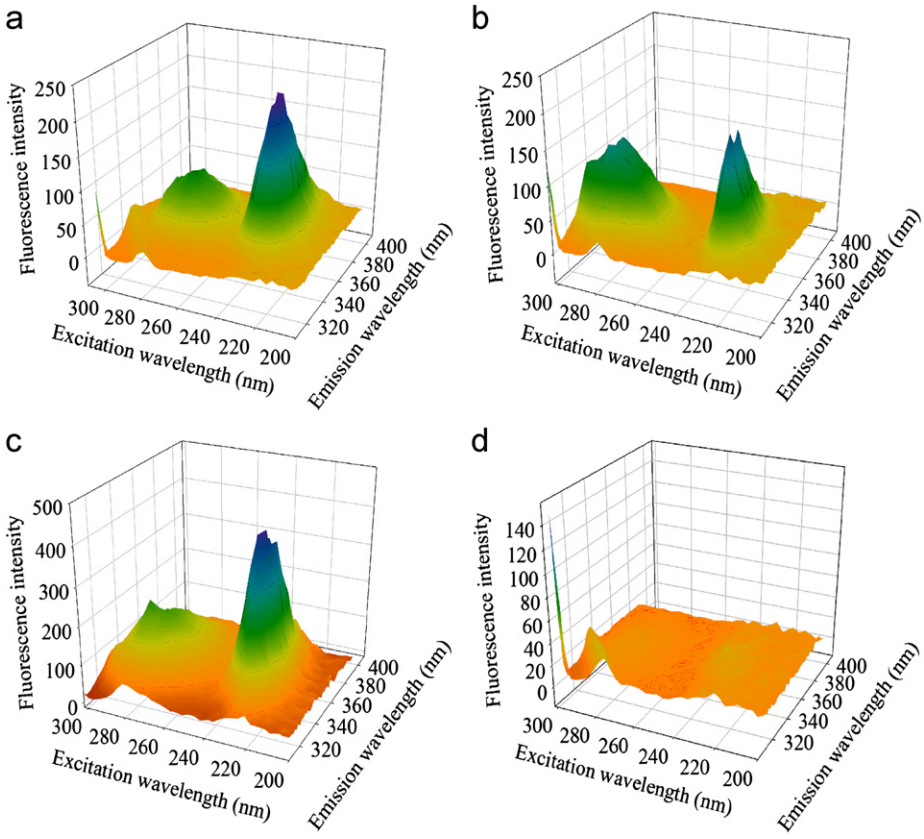


**Fig. 2.** Excitation–emission matrix fluorescence spectra for (a) pure NOA, (b) pure NAAME, (c) blank soil and (d) blank sewage sample.

**Table 3**
Results in prediction for reconstructed models using SWATLD after removing outlier samples.

| Reconstructed model | NOA | | | | NAAME | | | |
|---|---|---|---|---|---|---|---|---|
| | AR[a] | t-Test | RMSEP[b] | LOD[b] | AR[a] | t-Test | RMSEP[b] | LOD[b] |
| 1 | $97.0 \pm 3.4$ | 2.02[c] | 2.43 | – | $102.7 \pm 4.6$ | 1.24[c] | 4.51 | – |
| 2 | $100.4 \pm 4.9$ | 0.16[d] | 1.38 | 0.46 | $101.3 \pm 5.2$ | 0.42[d] | 5.42 | 1.56 |
| 3 | $88.1 \pm 2.1$ | 10.93[d] | 4.97 | 0.36 | $103.5 \pm 4.2$ | 1.46[d] | 1.71 | 1.32 |
| 4 | $92.2 \pm 3.0$ | 4.73[e] | 3.72 | 0.53 | $98.0 \pm 6.1$ | 0.70[e] | 8.06 | 1.38 |
| 5 | $104.5 \pm 6.8$ | 1.42[e] | 2.19 | 0.95 | $103.7 \pm 3.6$ | 2.17[e] | 3.25 | 2.69 |

[a] %.
[b] ng $mL^{-1}$.
[c] $t^{8}_{0.025} = 2.31$ .
[d] $t^{6}_{0.025} = 2.45$ .
[e] $t^{7}_{0.025} = 2.36$ .

It was clear that there were three outlier samples. After removing outlier samples, the results of elliptical joint confidence regions (EJCR) [30] for slope and intercept of the regression of NOA and NAAME data, respectively, by applying the SWATLD algorithm to analysis of reconstructed model 2 (Fig.4(b) and (d), green) indicated that the results did not present a significant difference at the level of 95% confidence and were satisfactory. The fourth line of Table 3 showed the statistical results in prediction for reconstructed model 2. The limits of detection (LODs) were estimated with the approach described in Ref. [31] according to the expression: $LOD = 3.3\sigma_0$, where $\sigma_0$ was the standard deviation in the predicted concentration of the analyte of interest in three analytes-free soil blank samples. The obtained LOD of 0.46 ng $mL^{-1}$ for NOA was lower than the value of 2.0 ng $mL^{-1}$ reported in literature [27]. The LOD for NAAME was 1.56 ng $mL^{-1}$. Here $T \le t^{6}_{0.025} = 2.45$, that suggested that the results for NOA and NAAME were accurate and reliable. These results also revealed that the second-order calibration method based on the SWATLD algorithm was capable to quantitatively analyze of NOA and NAAME in complex soil samples and the prediction quality of the method was satisfactory.

### 4.2.2. *Model for quantification of NOA and NAAME in sewage samples*

Matrix effect, such as inner filter effects or analyte–background interactions, was a problem for quantitative analysis, which would make quantitative results inaccurate or useless [32,33]. Model 3 was built to investigate the prediction quality of the method by analyzing sewage samples in the presence of matrix effect such as fluorescence quenching phenomenon.

In Fig. 4(a), it was apparent that all the predicted values for NOA (pink hexagon) located below the perfect fit line, and the poor NOA recovery was obtained (only $83.2 \pm 6.9\%$, the fifth line of Table 2).

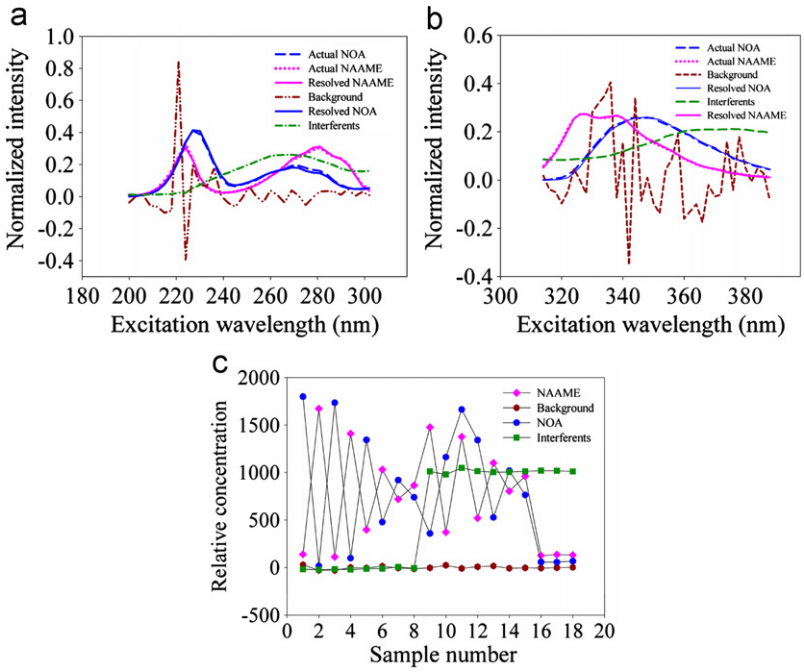


**Fig. 3.** Actual and resolved normalized excitation spectra (a), normalized emission spectra (b) and relative concentration profiles (c) of NOA and NAAME by applying SWATLD to analysis of reconstructed model 2.

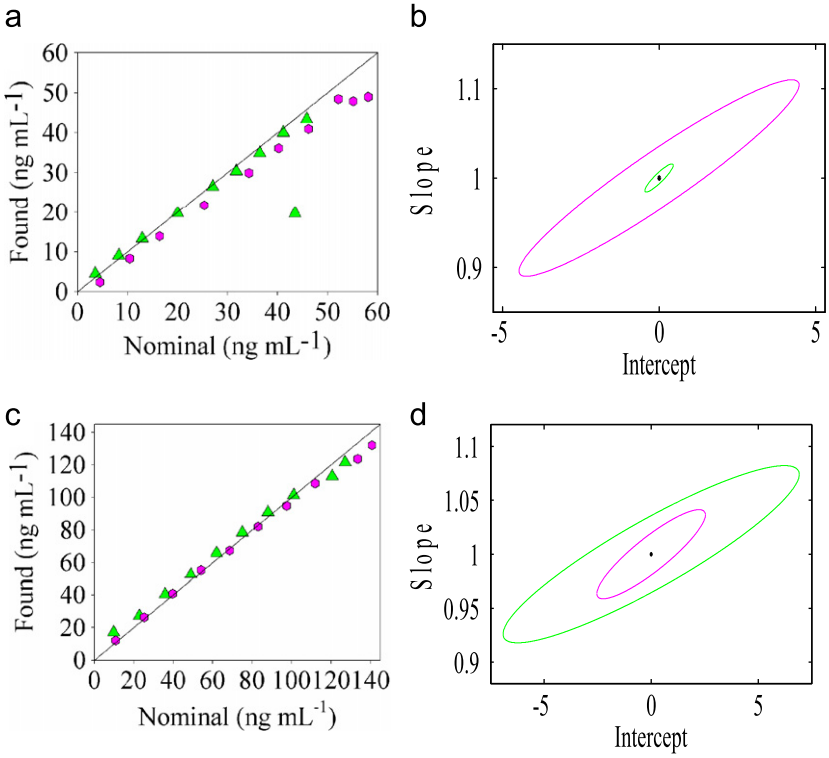


**Fig. 4.** Plots for the NOA (a) and NAAME (c) predicted concentrations in models 2 (green triangle up) and 3 (pink hexagon) as a function of the nominal values (the solid lines are the perfect fits), and elliptical joint confidence regions (EJCR, at 95% confidence level) for slope and intercept of the regression of the data after removing outlier samples, (b) for NOA and (d) for NAAME. The dots mark the theoretical (intercept=0, slope=1) point. (For interpretation of the references to colour in this figure legend, the reader is referred to the web version of this article.)

After removing outlier samples, here $T=10.93>t^{6}_{0.025}=2.45$ (the fifth line of Table 3), that also suggested that there was significant difference between the predicted values and the ideal value 100%. The EJCR for NOA in sewage sample (pink) was far bigger than the ones in soil sample (green) (Fig. 4(b)). This revealed that bad prediction results for NOA were obtained. The reason may be that some inorganic or organic compounds which may be possibly present in the sewage samples produced quenching matrix effect for acidic compound NOA in our analysis. So, it indicated that the prediction quality of the method was affected by the presence of matrix effect. But for NAAME, no significant deviation was observed between the actual and predicted values (Fig. 4(c) and (d), green).

The good statistical results obtained for the predicted NAAME concentration were shown in the fifth line of Table 3. The LOD for NAAME remained at the part-per-billion levels (1.32 ng $mL^{-1}$). These results revealed that the method was appropriate for the determination of NAAME in sewage samples.

### 4.3. Models based on different fluorescence spectrophotometers

The investigation of the performance of calibration methods based on different instrumental response is being recognized by the outside world [34–38]. But the investigation is mainly focus on two-way arrangements ($i \times j$ matrices), less work has been done with in the area for three-way data structures ($i \times j \times k$ tensors). For example, calibration made for EEMF spectra, it is unknown how is the prediction quality of second-order calibration method for models based on different instruments. So, models 4, 5 and 6 were built to investigate the prediction quality of the method based on taking spectroscopic measurements at different fluorescence spectrophotometers.

#### 4.3.1. Models based on F4500-1 and F4500-2

The three-dimensional plots of EEMF spectra of soil sample containing 45.8 ng $mL^{-1}$ NOA and 120.6 ng $mL^{-1}$ NAAME measured by F4500-1 (model 4) and F4500-2 (model 5), respectively, were shown in Fig. 5(a) and (b).

It could be observed that the two maps of the soil sample were not alike although containing the same concentration of analytes. The most noticeable was the intensity difference. The pixel at $\lambda_{ex}$ 224 nm/$\lambda_{em}$ 340 nm was 453.5 for F4500-1 (Fig. 5(a)) and $\lambda_{ex}$ 230 nm/$\lambda_{em}$ 328 nm was 209.9 for F4500-2 (Fig. 5(b)), respectively. There was a small concentration-response difference between F4500-1 and F4500-2. However, there was still a linear relationship between concentration and fluorescence response at each of the two fluorescence spectrophotometers.

Fig. 6(a) and (c) suggested that the predicted concentrations for two analytes in initial models 4 (red circle) and 5 (dark red ×) were close to the perfect fit line. After removing outlier samples, the ellipses for both analytes contained the ideal point (0, 1) (Fig. 6(b) and (d)), which showed that the reference values and the results obtained by the SWATLD algorithm did not present a significant difference at the level of 95% confidence.

The sixth and seventh line of Table 3 showed good statistical results of applying the SWATLD algorithm to analysis of reconstructed models 4 and 5. This indicated that models 4 and 5 were valid. It also confirmed that the good prediction quality of the method can be obtained when the concentration-response of analytes at different fluorescence spectrophotometers did not exceed their corresponding linear ranges.

#### 4.3.2. Model based on F4500-3

The soil sample containing 45.8 ng $mL^{-1}$ NOA and 120.6 ng $mL^{-1}$ NAAME was also measured at F4500-3 (model 6). The three-dimensional plot of its EEMF spectra was shown in Fig. 5(c). There was a significant difference in fluorescence intensity for F4500-3 with F4500-1 and F4500-2. The pixel at $\lambda_{ex}$ 227 nm/$\lambda_{em}$ 342 nm was 3298.0.

Fig. 7 showed excitation and emission spectra profiles of two analytes, which were resolved from different models using the SWATLD algorithm. It was clear that these spectra profiles fell into three categories. The profiles based on the same instrument (F4500-1) clustered together without spectra shift. But for the profiles obtained from the less sensitive instrument (F4500-2), there were significant excitation spectra red-shift and emission spectra blue-shift, and for the profiles obtained from the more sensitive instrument (F4500-3), the change was just opposite.

It was observed in Fig. 6(a) and (c), all of the predicted values for two analytes in model 6 (cyan square) located below the perfect fit line, and the poor analytes recoveries were obtained. From the eighth row of Table 2 could be seen, the average recoveries were only 76.2 ± 9.0% and 75.9 ± 7.0% for NOA and NAAME, respectively. The values of t-test, 5.05 for NOA and 6.01 for NAAME, were far greater than the ideal value 2.26. The RMSEPs were 10.46 ng $mL^{-1}$ for NOA and 16.55 ng $mL^{-1}$ for NAAME. These made it obvious that the obtained results were very bad and model 6 was invalid. This can be attributed to the concentration-response of analytes at F4500-3 exceeding their corresponding linear ranges, which led to model 7 deviating from the trilinear structure. So, very poor prediction results were obtained.

## 5. Conclusions

This study showed that an effective and inexpensive method for simultaneous determination of 2-naphthoxyacetic acid (NOA) and 1-naphthaleneacetic acid methyl ester (NAAME) in environmental samples was developed. It was based on the self-weighted alternating trilinear decomposition algorithm second-order calibration analysis of the excitation–emission matrix fluorescence spectra of NOA and NAAME. In order to investigate the prediction qualities of the proposed method, different strategies, such as taking spectroscopic measurements in the presence of different matrix interferents and at different fluorescence spectrophotometers, were introduced to build calibration models and comparisons among them were done subsequently. It was found that the prediction quality of the method was affected by the presence of matrix effect (for NOA in model 3) and the significant concentration-response difference at fluorescence spectrophotometer (in model 6). However, good results were obtained in models 1, 2, 4 and 5. Such a

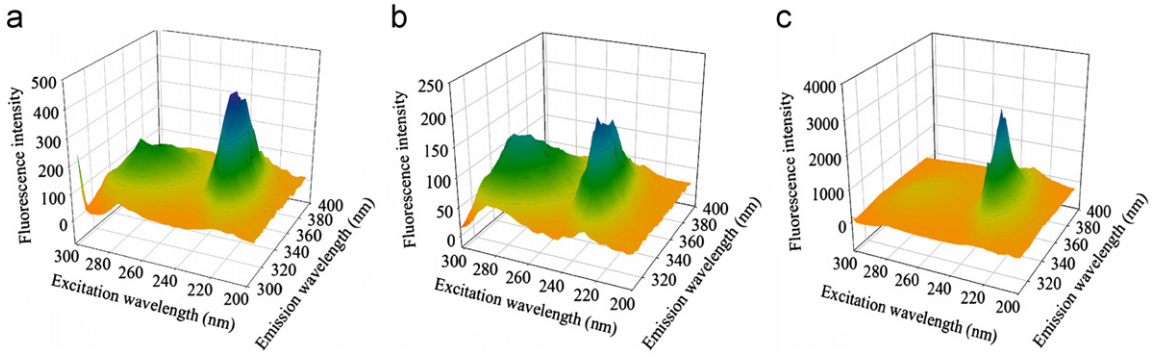


**Fig. 5.** Excitation–emission matrix fluorescence spectra of soil sample containing 45.8 ng $mL^{-1}$ NOA and 120.6 ng $mL^{-1}$ NAAME measured by three fluorescent spectrophotometers (a) F4500-1, (b) F4500-2 and (c) F4500-3, respectively.

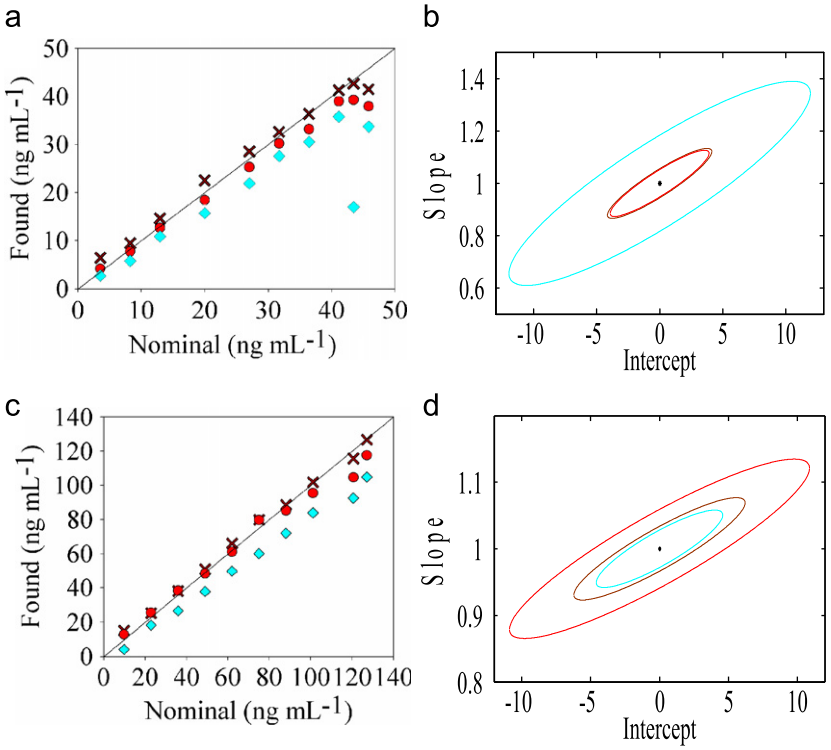


**Fig. 6.** Plots for the NOA (a) and NAAME (c) predicted concentrations in models 4 (red), 5 (dark red) and 6 (cyan) as a function of the nominal values (the solid lines are the perfect fits), and elliptical joint confidence regions (EJCR, at 95% confidence level) for slope and intercept of the regression of the data after removing outlier samples, (b) for NOA and (d) for NAAME. The dots mark the theoretical (intercept=0, slope=1) point. (For interpretation of the references to colour in this figure legend, the reader is referred to the web version of this article.)

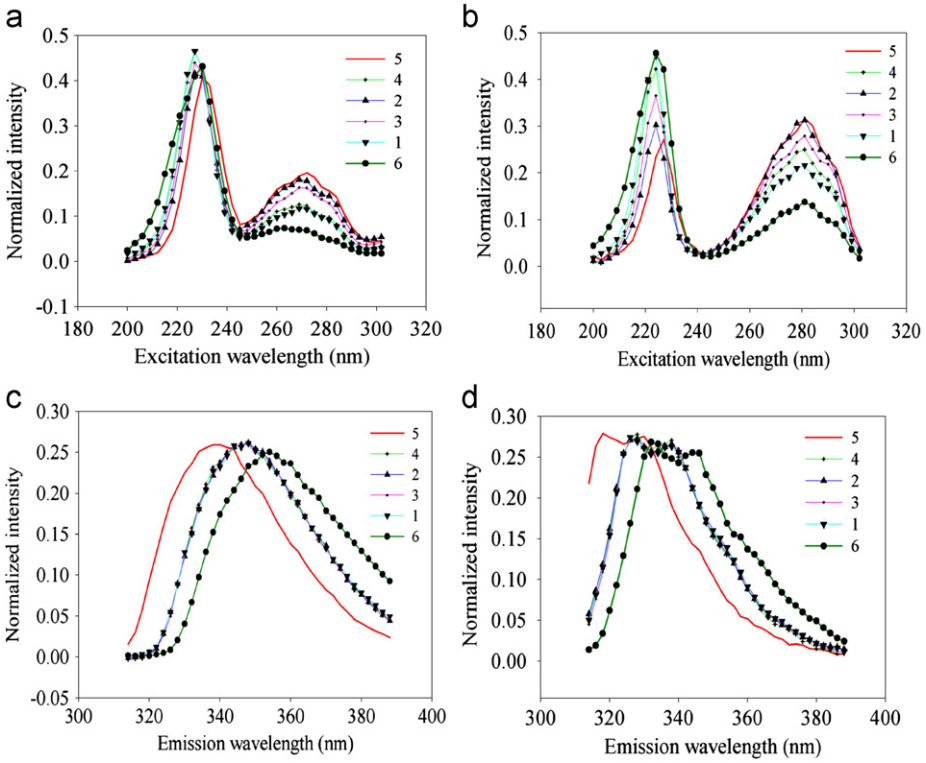


**Fig. 7.** Normalized excitation (a–b) and emission (c–d) profiles, which were resolved from different models (models 1–6) using SWATLD, respectively. a and c represent the spectral profiles of NOA, b and d denote the spectral profiles of NAAME.

chemometrics-based protocol may possess great potential to be extended as a promising alternative for more practical applications in environment monitoring and for the design of small intelligent and field-portable instruments that rely on statistical discrimination, not complete instrumental separation, of the target analytes even in the presence of unknown interferences.

## Acknowledgements

The authors gratefully acknowledge the National Natural Science Foundation of China (Grant no. 21175041), the National Basic Research Program (Grant no. 2012CB910602) and Program for Changjiang Scholars and Innovative Research Team in University (PCSIRT) for financial supports.

## References

[1] G.M. Escandar, A.C. Olivieri, N.M. Faber, H.C. Goicoechea, A. Muñoz de la Peña, R.J. Poppi, Trends Anal. Chem. 26 (2007) 752–765.
[2] H.L. Wu, J.F. Nie, Y.J. Yu, R.Q. Yu, Anal. Chim. Acta 650 (2009) 131–142.
[3] S. Mas, A. de Juan, R. Tauler, A.C. Olivieri, G.M. Escandar, Talanta 80 (2010) 1052–1067.
[4] P.W. Ryan, B. Li, M. Shanahan, K.J. Leister, A.G. Ryder, Anal. Chem. 82 (2010) 1311–1317.
[5] K.S. Booksh, B.R. Kowalski, Anal. Chem. 66 (1994) 782–791.
[6] X.D. Qing, H.L. Wu, Y.N. Li, C.C. Nie, J.Y. Wang, S.H. Zhu, R.Q. Yu, Anal. Methods 4 (2012) 685–692.
[7] R.A. Harshman, UCLA Working Papers in Phonetics vol. 16 (1970) pp. 1-84.
[8] E. Sánchez, B.R. Kowalski, Anal. Chem. 58 (1986) 496–499.
[9] E. Sánchez, B.R. Kowalski, J. Chemom. 4 (1990) 29–45.
[10] H.L. Wu, M. Shibukawa, K. Oguma, J. Chemom. 12 (1998) 1–26.
[11] Z.P. Chen, H.L. Wu, J.H. Jiang, Y. Li, R.Q. Yu, Chemom. Intell. Lab. Syst. 52 (2000) 75–86.
[12] A.L. Xia, H.L. Wu, D.M. Fang, Y.J. Ding, L.Q. Hu, R.Q. Yu, J. Chemom. 19 (2005) 65–76.
[13] E. Bezemer, S.C. Rutan, Chemom. Intell. Lab. Syst. 60 (2002) 239–251.
[14] M. Linder, R. Sundberg, Chemom. Intell. Lab. Syst. 42 (1998) 159–178.
[15] A.C. Olivieri, J. Chemom. 19 (2005) 253–265.
[16] V.A. Lozano, G.A. Ibañez, A.C. Olivieri, Anal. Chim. Acta 610 (2008) 186–195.
[17] A. García Reiriz, P.C. Damiani, M.J. Culzoni, H.C. Goicoechea, A.C. Olivieri, Chemom. Intell. Lab. Syst. 92 (2008) 61–70.
[18] D. Giménez, L. Sarabia, M.C. Ortiz, Anal. Chim. Acta 544 (2005) 327–336.
[19] Å. Rinnan, J. Riu, R. Bro, J. Chemom. 21 (2007) 76–86.
[20] Y.N. Li, H.L. Wu, X.D. Qing, C.C. Nie, S.F. Li, Y.J. Yu, S.R. Zhang, R.Q. Yu, Talanta 85 (2011) 325–332.
[21] A. Shahzad, M. Knapp, M. Edetsberger, M. Puchinger, E. Gaubitzer, G. Köhler, Appl. Spectrosc. Rev. 45 (2010) 92–99.
[22] J. Fitch, Application of Fluorescence Spectroscopy to Environmental Studies. University of Tennessee at Chattanooga, Chemistry, 2002.
[23] J. Sádecká, J. Tóthová, Czech J. Food Sci. 25 (2007) 159–173.
[24] Y.N. Li, H.L. Wu, J.F. Nie, S.F. Li, Y.J. Yu, S.R. Zhang, R.Q. Yu, Anal. Methods 1 (2009) 115–122.
[25] Y.N. Li, H.L. Wu, S.H. Zhu, J.F. Nie, Y.J. Yu, X.M. Wang, R.Q. Yu, Anal. Sci. 25 (2009) 83–88.
[26] J.A. Murillo Pulgarín, L.F. García Bermejo, I. Sánchez Ferrer Robles, S. Becedas Rodríguez, Phytochem. Anal. 29 (2011) 1099–1107.
[27] S. Casado Terrones, J.F. Fernández Sánchez, A. Segura Carretero, A. Fernández Gutiérrez, Sens. Actuators B: Chem. 107 (2005) 929–935.
[28] A.D. Ibrahim, A. Abubakar, A.A. Aliero, A. Sani, S.E. Yakubu, J. Pharm. Biomed. Sci. 1 (2011) 79–84.
[29] R. Bro, H.A.L. Kiers, J. Chemom. 17 (2003) 274–286.
[30] A.G. González, M.A. Herrador, A.G. Asuero, Talanta 48 (1999) 729–736.
[31] L.A. Currie, Anal. Chim. Acta 391 (1999) 105–126.
[32] M. Martínez Galera, T. López López, M.D. Gil García, J.L. Martínez Vidal, D. Picón Zamora, L. Cuadros Rodríguez, Anal. Bioanal. Chem. 375 (2003) 653–660.
[33] W.M.A. Niessen, P. Manini, R. Andreoli, Mass Spectrom. Rev. 25 (2006) 881–899.
[34] N. Lars, Chemom. Intell. Lab. Syst. 29 (1995) 283–293.
[35] R.N. Feudale, N.A. Woody, H. Tan, A.J. Myles, S.D. Brown, J. Ferré, Chemom. Intell. Lab. Syst. 64 (2002) 181–192.
[36] J. Thygesen, F. van den Berg, Anal. Chim. Acta 705 (2011) 81–87.
[37] M.R. Kunz, J.H. Kalivas, E. Andries, Anal. Chem. 82 (2010) 3642–3649.
[38] Z.P. Chen, L.M. Li, R.Q. Yu, D. Littlejohn, A. Nordon, J. Morris, A.S. Dann, P.A. Jeffkins, M.D. Richardson, S.L. Stimpson, Analyst 136 (2011) 98–106.